BMC Bioinformatics

DATABASE

Open Access

RCDRank: a web server to prioritize regulated cell death modalities

Nan Zhou[1†], Tong Yin[2,3†], Huiran Sun[2,3], Qiqi Luo[4], Yuhong Zhang[1], Xiaolei Shi[1], Jinku Bao[4*], Li Peng[2,3*] and Xiaoqing Yuan[2,3*]

[†]Nan Zhou and Tong Yin have contributed equally to this work.

*Correspondence:
Jinku Bao
baojinku@scu.edu.cn
Li Peng
pengli9@mail.sysu.edu.cn
Xiaoqing Yuan
yuanxq7@mail.sysu.edu.cn
[1]Research Center, The Affiliated Brain Hospital, Guangzhou Medical University, Guangzhou 510370, China
[2]Medical Research Center, Sun Yat-Sen Memorial Hospital, Sun Yat-Sen University, Guangzhou 510120, China
[3]Guangdong Provincial Key Laboratory of Malignant Tumor Epigenetics and Gene Regulation, Guangdong-Hong Kong Joint Laboratory for RNA Medicine, Sun Yat-Sen Memorial Hospital, Sun Yat-Sen University, Guangzhou 510120, China
[4]College of Life Science, Sichuan University, Chengdu 610064, China

Abstract

Background Regulated cell death (RCD) maintains cellular homeostasis and tissue integrity, playing a pivotal role in both health and disease. A variety of RCD subroutines have been identified, each characterized by distinct molecular and morphological features. These cell death modalities do not operate in isolation. Instead, they interact with one another in complex ways. This interaction leads to crosstalk through interconnected and often overlapping signaling pathways. Multiple forms of RCD can coexist within the same disease, influencing various cell types or even the same cell type either synchronously or sequentially. Understanding the intricate dynamics of RCD is of high importance. However, it is challenging to discern the relative contribution of various RCD modalities within the specific biological context. This necessitates the development of advanced methodologies to systematically analyze the priority of RCD pathways in various cellular environments.

Main In the present study, we first created a manually curated collection of gene sets for 18 well-characterized RCD modes. We then estimated the significance of each RCD pathway by combining the results of seven gene set enrichment tests via the Tippet *p*-value combination approach. Afterward, the consensus of enrichment for each RCD pathway across tests was evaluated using robust rank aggregation. The priorities of RCD were subsequently resolved by considering both the combined *p* value and the consensus score. The reliability of the proposed approach was validated by applying it to explore the RCD modes in intracranial aneurysms. Finally, a user-friendly web application was created for researchers worldwide.

Conclusion Our study offers a new way to reveal complicated RCD modalities in specific biological settings. The web server is freely accessible at https://www.zhounan.org/rcdrank.

Keywords Regulated cell death, Priority, Rank, Web server

Background

Regulated cell death (RCD) is a sophisticated biological mechanism fundamentally distinct from accidental cell death (ACD). Historically, scientific interest in RCD traces back to 1842 when dying cells were first observed in toads, but the field dramatically expanded in 1972 with the introduction of the term apoptosis [1]. Unlike ACD, which

results from uncontrolled injurious stimuli overwhelming cellular adaptive capacities, RCD represents a regulated form of cell death that can be modulated by specific genetic or pharmacological interventions [2]. RCD can either occur under physiological conditions or result from disruptions in cellular homeostasis caused by intracellular or extracellular disturbances [3, 4]. The former functions as an intrinsic component of physiological processes and is also known as programmed cell death (PCD) [5].

RCD is essential for maintaining human health and homeostasis. It is crucial for organism development, immune system regulation, and cell number control. The capacity for cells to self-eliminate in a controlled manner under specific conditions is vital for survival, as it prevents the propagation of harmful mutations and serves as an evolutionary strategy to maintain optimal cellular and tissue function [6]. Dysregulation of RCD can lead to severe health issues, including cancer, autoimmune diseases, and neurodegenerative disorders. For example, it is now evident that the first step in neuritic plaque formation in Alzheimer's disease is neuronal degeneration driven by iron overload and ferroptosis [7]. NLRP12- and NLRC4-induced GSDMD-dependent pyroptosis contributes to the pathogenesis of dry eye disease accompanied by IL-33 processing [8]. MELK regulates the levels of cuproptosis-related gene to promote drug resistance, alter mitochondrial function, and ultimately promote hepatocellular carcinoma progression [9].

RCD encompasses diverse modalities with distinct molecular signatures and unique morphological changes. Despite these differences, these modalities are interconnected through shared regulatory components and overlapping signaling pathways [10]. Key signaling molecules are often pleiotropic. This characteristic enables crosstalk between different cell death mechanisms and creates interrelations among various RCD forms. Different RCD subroutines can be activated simultaneously or sequentially in response to cellular stress, and they may operate in parallel within the same cells or across different cell types [11]. PANoptosis, a term coined for the simultaneous induction of pyroptosis, apoptosis and necroptosis, is a well-established example of this concept [12]. Interconnected RCD modalities may coexist within the same disease, affecting tissues through synchronous or sequential activation patterns at both the cellular and organismal levels [13]. RCD modalities share triggers, execution events, and protective mechanisms. One form can induce another [14]. This can occur within the same cell or in neighboring cells.

The final cell fate emerges from the interplay of various cell death programs. It is now evident that multiple RCD forms operate simultaneously in diseases such as cancer [15]. They function as interconnected backup mechanisms that enable tumor cells to switch death modalities when primary pathways are blocked. Crosstalk between RCD pathways also affects therapy. Therapeutic interventions should account for disease stage and context. In some settings, targeting secondary or alternative cell death modes may be more effective than targeting only the predominant pathways [16]. A comprehensive understanding of RCD interconnections is therefore essential for developing next-generation therapies that can overcome drug resistance and adapt to the dynamic nature of cellular death programs.

Although cell death is biologically important, the dominant or involved forms of RCD can vary greatly across diseases, genetic perturbations, drug treatments, and stress responses. This diversity makes it challenging to determine which RCD pathways are associated with a specific context. It also makes it hard to distinguish major RCD forms

from minor ones. Moreover, purchasing all known RCD agonists or inhibitors is neither practical nor cost-effective. To address this, we aimed to develop a practical and economical approach for identifying RCD modes actively involved in a specific cellular environment. In this study, we constructed a manually curated gene set collection for RCD. We then developed a novel approach to prioritize RCD modalities across diverse biological contexts using transcriptomic profiling data. To facilitate accessibility and usability, we also established the RCDRank web server, which offers an intuitive interface and comprehensive visualization features.

Construction and content

Preparing RCD genes

Over the past few decades, various types of RCD have been identified. This study includes RCD modalities primarily defined by the Nomenclature Committee on Cell Death (NCCD) [17]. For those not covered by the NCCD, we used definitions from Tang et al. as a complement [18]. Although cuproptosis and disulfidptosis are too new to be defined in either source, we included them based on our review of recent articles [19, 20]. Hence, we collected the gene sets for a total number of 18 RCD subroutines, including autophagy-dependent cell death (ADCD), alkaliptosis, apoptosis, autosis, cuproptosis, disulfidptosis, entotic cell death, ferroptosis, immunogenic cell death, lysosome-dependent cell death, mitotic death, mitochondrial permeability transition (MPT)-driven necrosis, necroptosis, NETotic cell death, oxeiptosis, parthanatos, pyroptosis, and regulated necrosis.

We used the same strategy as in our previous work to collect RCD gene sets [21]. Briefly, we obtained genes from public repositories such as Gene Ontology and Kyoto Encyclopedia of Genes and Genomes (KEGG) [22–26]. We then manually classified them as drivers, suppressors, markers, or unclassified genes [27]. For RCD types not included in public repositories, genes were manually curated from original publications reporting wet-lab experiments. Articles were searched in PubMed using the RCD name as a keyword. Each gene entry was annotated directly based on the evidence presented in its source publication. A rigorous cross-checking protocol was implemented to ensure the highest standard of data accuracy. Finally, the collected gene sets were formatted into a '.gmt' file, a widely adopted common format for functional enrichment analysis (FEA).

Prioritizing RCD modalities

Gene set enrichment test (a.k.a., FEA) is an efficient method to obtain meaningful biological insights from regulated expression profiles. Over-representation analysis (ORA) and functional class scoring (FCS) are two popular categories of FEA methods [28]. To identify RCD events with varying priorities in a specific biological context, we developed a method that ranks RCD pathways through enrichment analysis. Seven FEA methods were employed, incorporating both ORA- and FCS-based approaches. The ORA-based methods include hypergeometric test and Enrichr, and the FCS-based methods include GSEA, GSEA prerank, GOAT, ssGSEA, and GSVA [29–31]. Notably, we did not apply topology-based methods because the required pathway topology information is unavailable in current data sets.

To prioritize RCD modalities for a given data set, such as a list of differentially expressed genes (DEGs), the following steps are used. Initially, each method

independently assesses the enrichment of RCD pathways and calculates adjusted *p*-values. Subsequently, the Tippett's method combines individual *p*-values across methods to obtain a single combined *p*-value [32]. Next, RCD pathways are ranked based on individual *p*-values, and the robust rank aggregation algorithm aggregates the rankings across methods to estimate a consensus score. This score reflects how consistently each pathway is enriched across methods. Finally, the priority of RCD pathways is determined by considering both the combined *p*-value and the consensus score. The lower the combined *p*-value and the consensus enrichment score, the greater the priority of the RCD pathway. The process is illustrated in Fig. 1.

Development and deployment

The back end server handles analysis jobs. It was built using Python (3.11.12) and R (4.3.1) scripts. The development process integrated several libraries and packages, including DESeq2 (1.42), limma (3.58), GOAT (1.1.2), RobustRankAggreg (1.2.1), pandas (2.2.3), plotly (6.1.1), and gseapy (1.1.8). These components play a vital role in enhancing the overall functionality and performance of the server, ensuring robust and efficient analysis capabilities.

The front end web interface was crafted using HTML5, CSS3, and JavaScript. To streamline the development process and ensure a seamless user experience, a suite of powerful tools and frameworks was employed. These include Bootstrap, jQuery, DataTables, and Plotly. The service runs on an AWS EC2 instance, with an Apache2 web server optimized for Ubuntu.

Statistics of RCD genes.

As depicted in Fig. 2A, we compiled gene sets for 18 RCD pathways. In total, there are 2802 unique RCD genes. The number of genes varies significantly across RCD pathways, ranging from as few as 6 to as many as 2078. Specifically, apoptosis has the highest number of genes, while oxeiptosis has the lowest. The remaining RCD types encompass genes numbering from 11 to 564.

As shown in Fig. 2B, protein-coding genes constitute the largest group, with a total of 2561 genes, reflecting their predominant role in the genome. The NA category, representing genes with unassigned or unknown classifications, is the second most abundant, comprising 169 genes. Non-coding RNA genes follow, including 47 miRNA genes, 21

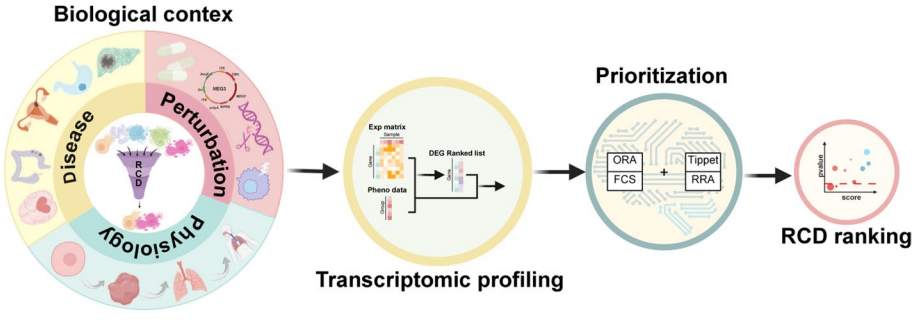

Fig. 1 Schematic workflow of the analytical framework. It aims to identify multiple RCD modalities that are active within specific biological contexts, with a focus on disease, perturbation, and physiological states as the most common scenarios. Transcriptomic data are utilized to prioritize RCD modalities by integrating enrichment analysis results from various methods through amalgamation techniques. The final ranking of RCD modalities is determined by evaluating both the significance levels and the consensus of enrichment across methods

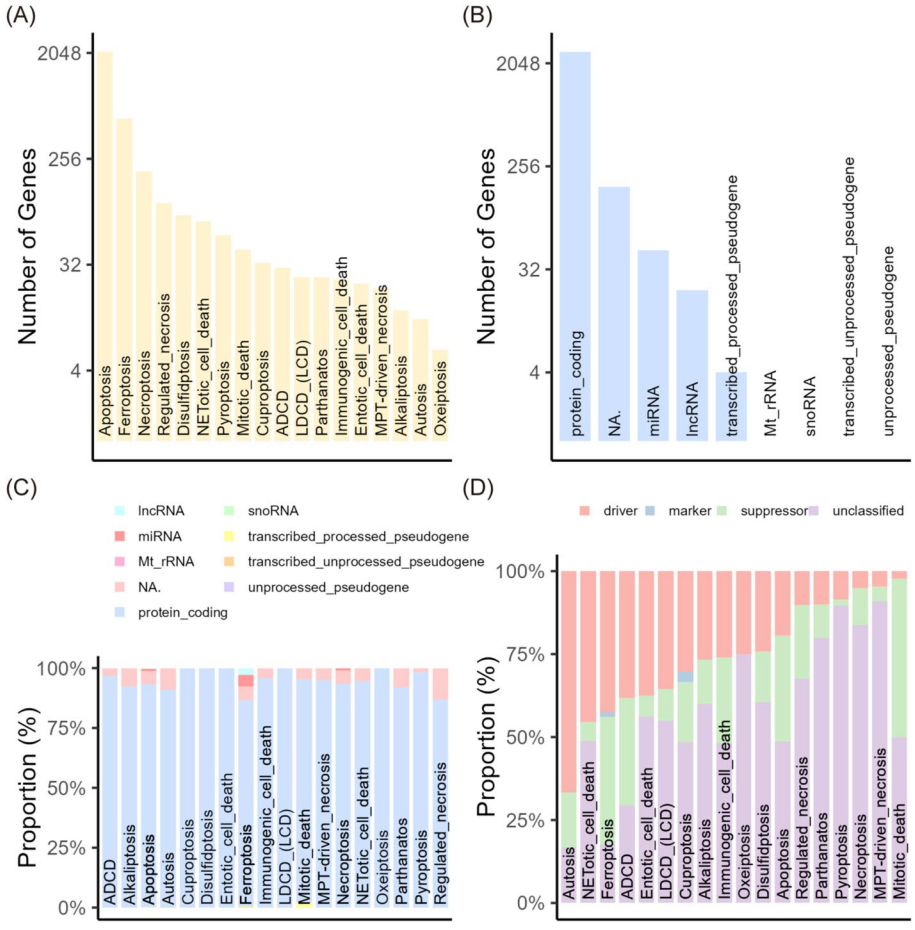

Fig. 2 Statistic description of genes within RCD pathways. **A** The distribution of gene counts across various types of RCD. **B** The distribution of genes across various gene types. **C** The proportional composition of various gene types across RCD subroutines. **D** The composition of driver, suppressor, marker, and unclassified genes across RCD modalities

lncRNA genes, and 4 transcribed processed pseudogenes. The remaining gene categories are represented by only one gene.

The composition of gene types also exhibits some variation across different RCD modalities (Fig. 2C). Protein-coding genes constitute the predominant gene category across all RCD modalities. Notably, the category labeled as NA exhibits a non-negligible proportion in several RCD types, including ADCD, alkaliptosis, apoptosis, autosis, ferroptosis, immunogenic cell death, mitotic death, MPT-driven necrosis, necroptosis, NETotic cell death, parthanatos, pyroptosis, and regulated necrosis. Other gene categories generally represent only a minor fraction of the overall gene composition. Of particular interest, ferroptosis displays a distinct profile characterized by a notable proportion of lncRNAs and miRNAs.

RCD genes were stratified into four distinct functional classifications: driver, suppressor, marker, and unclassified genes (Fig. 2D). Marker genes consistently represent the smallest proportion, and they are even absent in some RCD types. Autosis stands out with the highest proportion of driver genes, while mitotic death demonstrates the lowest driver gene representation. Conversely, mitotic death is characterized by the most suppressor genes, while pyroptosis exhibits the fewest suppressor genes. MPT-driven

necrosis and pyroptosis share a remarkably similar and predominant proportion of unclassified genes. This large uncharacterized component suggests significant knowledge gaps in our understanding of them. In contrast, autosis demonstrates the smallest fraction of unclassified genes. These differences reflect an uneven level of exploration across RCD types, highlighting a critical need for targeted research to elucidate the genetic basis more completely.

Web interface

On the website, the navigation bar links to all resources (Fig. 3A). The 'Home' link opens the landing page, and the 'Analysis' link opens the tool page where users can prioritize RCD pathways using their experimental data. The analysis page is organized into a series

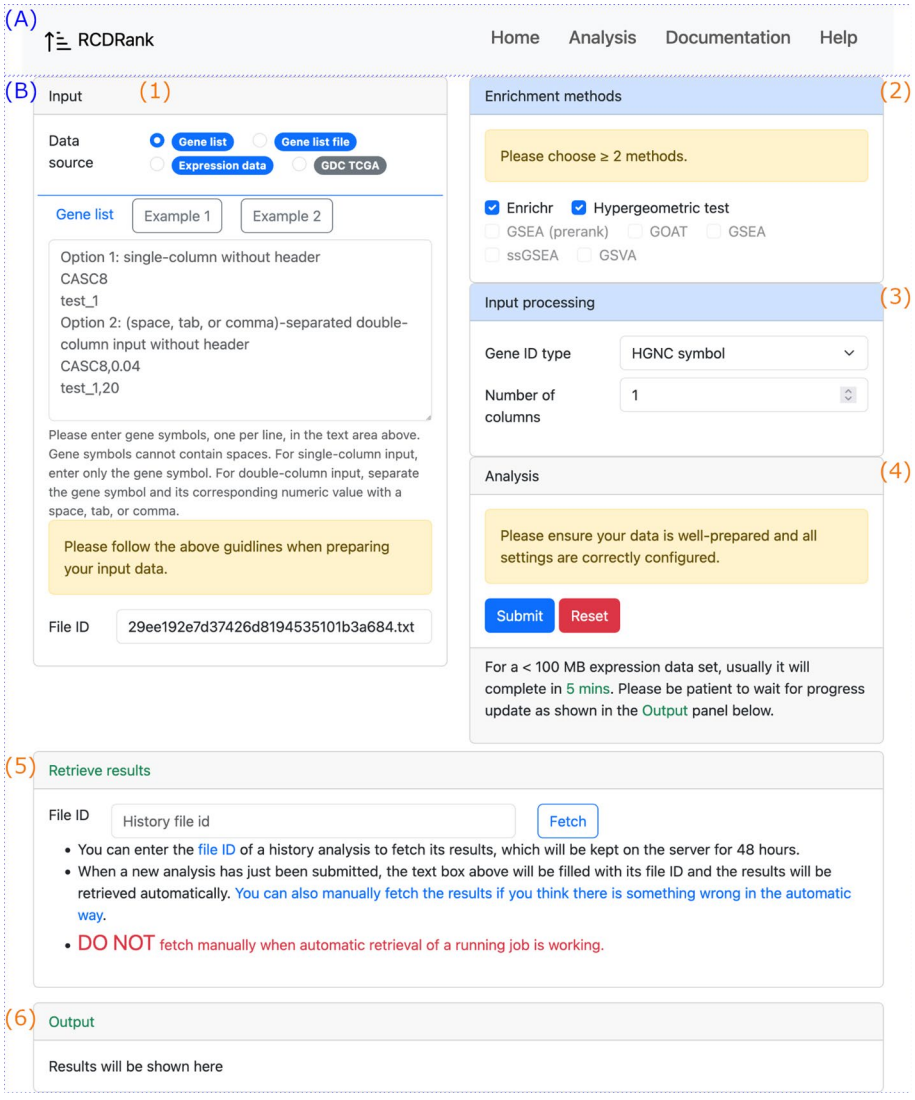

Fig. 3 Overview of the user interface. **A** Screenshot of the navigation bar showing links to all resources on the website. **B** Screenshot of the 'Analysis' tool page. (B1) The 'Input' panel where various types of data can be accepted as input. (B2) The 'Enrichment methods' panel to select the methods that will be used during the analysis. (B3) The 'Input processing' panel for preprocessing of the input data. (B4) The 'Analysis' panel providing options to submit or reset the analysis. (B5) The 'Retrieve results' panel for accessing past analyses. (B6) The 'Output' panel displaying comprehensive results ready for export. Please note that for different data sources, as indicated in (B1), the content in (B2) and (B3) will vary

of panels, each with distinct functionality, designed to be informative and intuitive. The 'Input' panel is where users upload their data, with clear instructions on data preparation provided. The parameter configuration panels are located to the right of the 'Input' panel and are dependent on the input provided. For instance, Fig. 3B illustrates settings for gene list input. When the input changes, the settings adjust accordingly (not shown). The 'Retrieve results' panel enables users to retrieve history results from the server within the last 48 hours using the analysis identifier, known as the file identifier. All results from a completed analysis are displayed in the 'Output' panel, where they can be visually examined and exported to local storage.

Accuracy and reliability

To demonstrate the accuracy and reliability of RCDRank, we utilized it to reanalyze the RCD pathways implicated in the pathogenesis of intracranial aneurysms (IA), as previously explored by Zhu et al. [33]. They identified apoptosis, necroptosis and pyroptosis as being associated with IA pathogenesis. Here, we reproduced these established scientific findings via RCDRank.

We acquired RNA-seq data for IA from the Gene Expression Omnibus (GEO) with the accession number GSE122897 [34]. The accompanying platform annotation and phenotypic data were also downloaded. This data set was derived from 44 IA samples and 16 control samples of the intracranial cortical artery. The raw counts matrix was downloaded and gene identifiers were converted to official HGNC symbols.

We conducted the analysis using RNA-seq data as input. The 'Data source' parameter was set to 'Expression data'. After uploading the data, the analysis was executed with default parameters. In the background, differential gene expression analysis was performed using a cutoff of fold change (FC) > 2 and $p < 0.05$. These thresholds provide a robust balance between sensitivity and specificity, adhering to established conventions in the field [35]. The results show that NETotic cell death, pyroptosis, and apoptosis were significantly enriched RCD pathways in IA (Fig. 4A).

The DEG step also produced a gene list ranked by log2-transformed fold change values. We then utilized this gene list as input for a second analysis, setting the 'Data source' parameter to 'Gene list file'. After uploading the data and specifying 'Number of columns' as 2, the analysis was performed without altering any other parameters. The

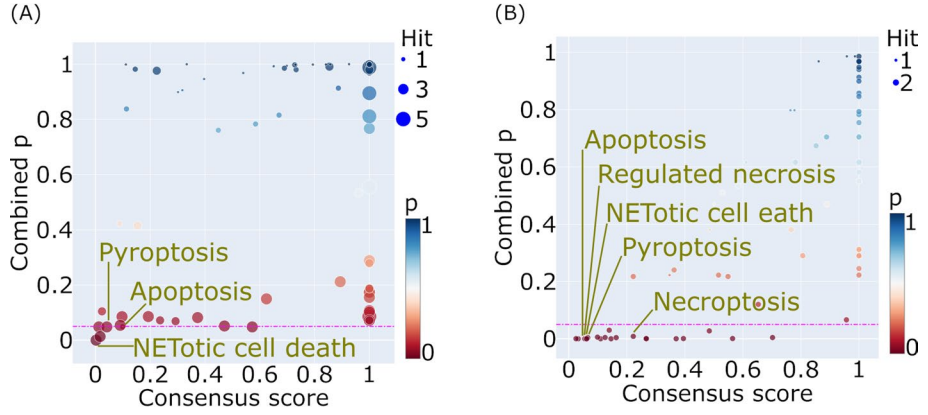

Fig. 4 Validation by recapitulating RCD modes in the pathogenesis of IA. **A** Enriched RCD pathways in IA derived from the raw RNA-seq count matrix. **B** Enriched RCD pathways in IA based on a gene list sorted by log2 fold change values

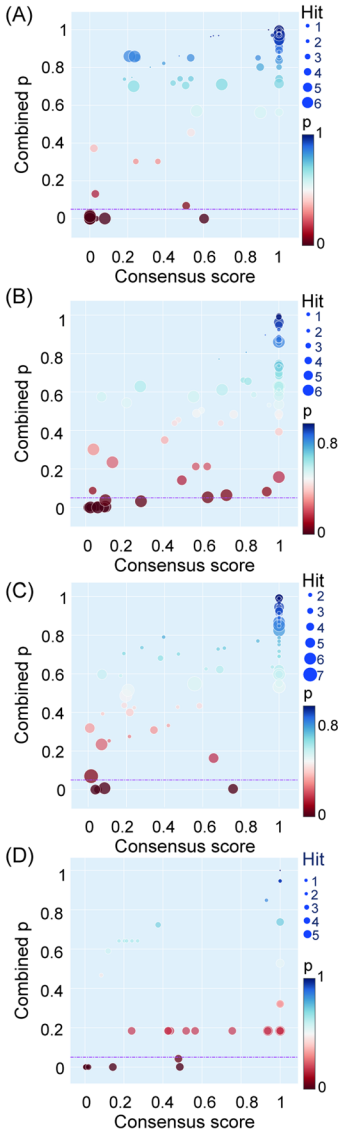

RCD	Combined p	Consensus score
Apoptosis	0.00	0.02
NETotic_cell_death	0.00	0.00
Ferroptosis_unclassified.reg.	0.00	0.00
Apoptosis_unclassified	0.00	0.03
Ferroptosis	0.00	0.01
Apoptosis_suppressor	0.00	0.02
Apoptosis_driver	0.00	0.60
Ferroptosis_suppressor	0.00	0.08
NETotic_cell_death_unclassified	0.01	0.00
ADCD	0.02	0.00

RCD	Combined p	Consensus score
Apoptosis	0.00	0.02
Apoptosis_driver	0.00	0.01
Apoptosis_unclassified	0.00	0.02
Ferroptosis_unclassified.reg.	0.00	0.06
Apoptosis_suppressor	0.00	0.04
Ferroptosis	0.00	0.10
Ferroptosis_suppressor	0.00	0.02
Disulfidptosis	0.00	0.10
Disulfidptosis_unclassified.reg.	0.01	0.06
Necroptosis_unclassified	0.03	0.29
Necroptosis	0.04	0.10

RCD	Combined p	Consensus score
Apoptosis	0.00	0.05
Apoptosis_suppressor	0.00	0.04
Apoptosis_unclassified	0.00	0.76
Apoptosis_driver	0.01	0.09

RCD	Combined p	Consensus score
Apoptosis	0.00	0.00
Ferroptosis	0.00	0.02
Apoptosis_unclassified	0.00	0.02
Ferroptosis_unclassified.reg.	0.00	0.14
Apoptosis_suppressor	0.00	0.00
Apoptosis_driver	0.00	0.01
Ferroptosis_suppressor	0.00	0.49
Ferroptosis_driver	0.04	0.48

Fig. 5 Application cases. **A** Significantly perturbed RCD modalities in OA. **B** RCD triggered by arginine deprivation. **C** RCD involved in ROCK1 knockdown in smooth muscle cells. **D** RCD involved in response to cisplatin treatment

results showcase significantly enriched RCD pathways were apoptosis, regulated necrosis, NETotic cell death, pyroptosis, and necroptosis (Fig. 4B).

Utility and discussion

Here, we demonstrate the utilization of RCDRank on transcriptomic data derived from four common scenarios, namely disease pathogenesis, stress response, gene perturbation, and drug treatment. The results show that RCDRank is suitable for a wide range of basic and clinical research scenarios.

For the scenario of disease pathogenesis, we used RCDRank to identify RCD modes in osteoarthritis (OA) progression. The expression data were downloaded from GEO under accession number GSE114007. For the analysis, a fold change threshold of FC > 2 and a *p*-value threshold of $p < 0.05$ were applied. The results identify that apoptosis, ferroptosis, NETotic cell death, and ADCD were significantly dysregulated (Fig. 5A).

For the scenario of stress response, we clarified the various types of RCD associated with the response of retinoblastoma cells to arginine deprivation. The RNA-seq data were downloaded from GEO under accession number GSE278276. For the analysis, we applied a fold change threshold of FC > 1.5 and a significance threshold of $p < 0.05$. The results show apoptosis, ferroptosis, disulfidptosis and necroptosis are significantly involved (Fig. 5B).

For the scenario of gene perturbation, we explored RCD involved in ROCK1 knockdown in smooth muscle cells. The data were downloaded from GEO under accession number GSE56819. For the analysis, a fold change threshold of FC > 2 and a p-value threshold of $p < 0.05$ were applied. The results find apoptosis was significantly enriched (Fig. 5C).

For the scenario of drug treatment, we identified RCD associated with cisplatin response of MMP3-siRNA-treated HGSOC cells. RNA-seq data were downloaded from GEO with accession number GSE275051. For the analysis, we applied a fold change threshold of FC > 1.2 and a significance threshold of $p < 0.01$. The results show apoptosis and ferroptosis were enriched (Fig. 5D).

The field of FEA is still in an actively growing and improving stage, without a unified method or a gold standard [36]. Different tools could yield varying results. The amalgamation of methods demonstrated superior performance over a single method in gene set enrichment tests [37]. This prompts the exploration of combining multiple methods. However, simple intersection of multiple results yields conservative outcomes and overlooks vital information. In order to address this shortcoming and provide an efficient and accurate analysis framework, we have chosen to use p-value combination and robust rank aggregation to integrate outputs from different FEA methods. The validity of FEA is dependent upon rigorous statistical methods as well as accurate and up-to-date gene functional annotations. Hence we also developed a manually curated gene set collection for RCD, which is of high quality and ensures reliable enrichment analysis.

Several methods are available for p-value combination, such as Fisher's method, Pearson's method, Mudholkar and George's method, Stouffer's method, and Tippett's method [38]. Fisher's method gives the most weight to strongly significant results. Pearson's method is the reverse of Fisher's and focuses on large p-values. Stouffer's Z-score method finds consistent trends across all tests. Mudholkar and George's method compromises between the extremes of Fisher's and Pearson's methods. Tippett's method uses the smallest p-value to detect if at least one test is significant. We chose Tippett's method as it is better at detecting sparse signals [39]. Since different enrichment analysis methods could generate remarkably varied results, true effects are likely found in only a small number of tests [40]. This makes Tippett's method a suitable choice for our study, as it helps ensure that a single significant finding is not obscured by non-significant results in other tests.

The public validation datasets used in the present study have neither been incorporated into previous RCD prioritization frameworks nor subjected to similar studies. These datasets are valid independent test sets and enable an objective and comprehensive validation of the applicability and reliability of RCDRank.

We have validated the accuracy and reliability of RCDRank via a comprehensive reanalysis of RCD pathways implicated in the pathogenesis of IA, building upon the foundational work previously established by Zhu and colleagues [33]. In their study,

they identified differentially expressed genes between the IA and control groups. They also demonstrated that several RCD modalities, specifically apoptosis, necroptosis, and pyroptosis, play critical roles in IA development and progression. We successfully recapitulated the RCD types identified in the original investigation, thereby providing reciprocal validation of both sets of results (Fig. 4). This concordance with prior literature validates the sensitivity of RCDRank for investigating RCD-mediated disease mechanisms. Our analysis additionally identified that NETotic cell death is involved in IA pathogenesis. This suggests that IA may extend beyond apoptosis to encompass a broader spectrum of RCD modalities. A close association between ferroptosis and IA has also been independently confirmed by recent studies [41, 42]. Consistent with this, ferroptosis was significantly enriched in our analysis ($p < 0.001$). Collectively, these results suggest that RCDRank can help capture known RCD mechanisms and may aid in elucidating additional candidate modalities in complex diseases.

We demonstrated the applicability of RCDRank across four scenarios that typically involve shifts in RCD subroutines (Fig. 5). In the disease setting, we identified ferroptosis as one of the most prominently enriched death modes in OA, consistent with Miao et al. [43]. In the context of stress, we corroborated that arginine deprivation in retinoblastoma cells activates apoptosis and additionally identified an enrichment of other RCD types [44]. For genetic perturbation, we investigated the effect of ROCK1 knockdown and successfully prioritized apoptosis, a death pathway known to be regulated by ROCK1 [45]. Finally, in the drug treatment scenario, we investigated cisplatin exposure and successfully identified apoptosis as a major RCD form induced by this well-established apoptosis inducer [46]. In the disease and stress scenarios, enrichment of multiple RCD types beyond those previously reported suggests greater complexity. It may reflect the coexistence or interaction of different cell death programs within these biological settings. In contrast, the RCD patterns observed under single genetic perturbation or drug treatment were more specific, with fewer enriched RCD types. This likely reflects the more targeted nature of these interventions compared to the systemic complexity seen in disease and stress contexts.

RCDRank distinguishes itself from general platforms (e.g., Enrichr, GSEA) by focusing exclusively on manually curated, high-confidence RCD gene sets. Unlike standard tools, which typically use a single statistical approach, RCDRank integrates multiple approaches using p-value combination and RRA to improve robustness. Furthermore, RCDRank addresses the limitations of existing specialized databases, which are often constrained by narrower RCD coverage or restricted analytical functionality. Together, these features reflect RCDRank's novelty in quantitatively prioritizing RCD modalities.

Even though RCDRank is reliable to prioritize RCD modalities, we have to acknowledge that it shares some of the limitations derived from ORA and FCS methods. They assume gene independence, when in reality, gene products interact through complex networks in biological systems. This may limit our understanding of these interactions during expression changes. They also analyze pathways independently, whereas pathways often exhibit interdependencies. This ignores that genes often participate in multiple pathways, leading to overlooked pathway interactions and overlaps.

Conclusions

In the present study, we initially constructed a high-quality collection of gene sets for 18 RCD subroutines. We then developed an analytical framework to discern the priorities of RCD by integrating outputs from seven gene set enrichment tests. Utilizing p-value combination and robust rank aggregation, we estimated a combined *p*-value and a consensus enrichment score for each RCD modality. We used these two metrics to rank RCD modalities. This dual-criteria approach is intended to improve the robustness of the prioritization and to support subsequent experimental validation and therapeutic targeting. Finally, we developed a free web server, RCDRank, for easy access and use. RCDrank addresses a critical gap in RCD research: the lack of practical tools to determine which RCD types are functionally important in a specific biological context. Testing every known RCD modulator is costly and labor-intensive. Our approach enables researchers to make data-driven decisions by leveraging transcriptomic profiles. To ensure the long-term sustainability of the platform, we have established a dedicated maintenance team responsible for conducting iterative optimizations on a biannual basis. Future updates will focus on integrating the latest research advancements, enhancing algorithmic efficiency, and resolving technical issues. Beyond RCD, this study provides a conceptual and methodological paradigm for tackling similar challenges in other multifaceted biological systems. Metabolic pathways, RNA modifications, and post-translational modifications consist of numerous mechanistically diverse subtypes, and many are biologically important. However, it is often difficult to determine which subtype is most relevant in a given setting. RCDRank exemplifies how integrative, transcriptome-based analysis can guide the functional dissection of complex processes, paving the way for analogous tool development in other domains of biology.

Acknowledgements

We would like to express our sincere gratitude to the open-access data, software, and tools from public repositories for providing open access to valuable resources that significantly contributed to our research.

Author contributions

NZ: Methodology, Software, Writing—Original Draft. TY: Methodology, Software, Data Curation. HS: Formal analysis, Data Curation. QL: Investigation, Visualization. YZ: Validation. XS: Validation. JB: Resources, Writing—Review & Editing. LP: Conceptualization, Writing—Review & Editing, Supervision, Project administration, Funding acquisition. XY: Conceptualization, Writing—Review & Editing, Supervision, Project administration, Funding acquisition.

Funding

This work was supported by the National Natural Science Foundation of China [82372617 to L.P., 81803636 to X.Y.]; National Natural Science Foundation of China Major Research Program Cultivation Project [92578122 to J.B.]; Guangdong Basic and Applied Basic Research Foundation [2024B1515020090 and 2023A1515012683 to L.P., 2024A1515030038 and 2023A1515140033 to X.Y.]; Guangzhou Medical University Research Enhancement Project [50010724-1158 to N.Z.]; Basic and Applied Basic Research of Guangzhou Municipal Basic Research Plan [2024A03J0845 and 2023A04J2098 to L.P.]; Fundamental Research Funds for the Central Universities, Sun Yat-sen University [24ykqb004 to L.P.]; The Science and Technology Planning Project of Guangdong Province [2023B1212060013, 2020B1212030004]; Guangzhou Key Clinical Specialty (Clinical Medical Research Institute).

Data availability

The data generated during the current study are available at the project's website. Public datasets for the validation and application purposes are available from the GEO database with accession numbers GSE122897, GSE114007, GSE278276, GSE56819, and GSE275051. The source code has been deposited on GitHub at https://github.com/zhounandotorg/rcdrank.

Declarations

Ethics approval and consent to participate

Not applicable.

Consent for publication

Not applicable.

Competing interests

The authors declare that they have no competing interests.

Received: 19 August 2025 / Accepted: 16 March 2026
Published online: 26 March 2026

References

1. Zhang Y, Yi S, Luan M. Advances in non-apoptotic regulated cell death: implications for malignant tumor treatment. Front Oncol. 2025;15:1519119. https://doi.org/10.3389/fonc.2025.1519119.
2. Zhang W, Zhu Y, Liu H, Zhang Y, Liu H, Adegboro AA, et al. Pan-cancer evaluation of regulated cell death to predict overall survival and immune checkpoint inhibitor response. Npj Precis Oncol. 2024;8:1–21. https://doi.org/10.1038/s41698-024-00570-5.
3. Fuchs Y, Steller H. Programmed cell death in animal development and disease. Cell. 2011;147:742–58. https://doi.org/10.1016/j.cell.2011.10.033.
4. Galluzzi L, Bravo-San Pedro JM, Kepp O, Kroemer G. Regulated cell death and adaptive stress responses. Cell Mol Life Sci. 2016;73:2405–10. https://doi.org/10.1007/s00018-016-2209-y.
5. Galluzzi L, Bravo-San Pedro JM, Vitale I, Aaronson SA, Abrams JM, Adam D, et al. Essential versus accessory aspects of cell death: recommendations of the NCCD 2015. Cell Death Differ. 2015;22:58–73. https://doi.org/10.1038/cdd.2014.137.
6. Yu G, Klionsky DJ. Life and death decisions-the many faces of autophagy in cell survival and cell death. Biomolecules. 2022;12:866. https://doi.org/10.3390/biom12070866.
7. Streit WJ, Phan L, Bechmann I. Ferroptosis and pathogenesis of neuritic plaques in Alzheimer disease. Pharmacol Rev. 2025;77:100005. https://doi.org/10.1124/pharmrev.123.000823.
8. Chen H, Gan X, Li Y, Gu J, Liu Y, Deng Y, et al. NLRP12- and NLRC4-mediated corneal epithelial pyroptosis is driven by GSDMD cleavage accompanied by IL-33 processing in dry eye. Ocul Surf. 2020;18:783–94. https://doi.org/10.1016/j.jtos.2020.07.001.
9. Li Z, Zhou H, Zhai X, Gao L, Yang M, An B, et al. MELK promotes HCC carcinogenesis through modulating cuproptosis-related gene DLAT-mediated mitochondrial function. Cell Death Dis. 2023;14:733. https://doi.org/10.1038/s41419-023-06264-3.
10. Shen S, Shao Y, Li C. Different types of cell death and their shift in shaping disease. Cell Death Discov. 2023;9:1–12. https://doi.org/10.1038/s41420-023-01581-0.
11. Lee E, Song C-H, Bae S-J, Ha K-T, Karki R. Regulated cell death pathways and their roles in homeostasis, infection, inflammation, and tumorigenesis. Exp Mol Med. 2023;55:1632–43. https://doi.org/10.1038/s12276-023-01069-y.
12. Malireddi RKS, Kesavardhana S, Kanneganti T-D. ZBP1 and TAK1: master regulators of NLRP3 inflammasome/pyroptosis, apoptosis, and necroptosis (PAN-optosis). Front Cell Infect Microbiol. 2019;9:406.
13. D'Amico M, De Amicis F. Challenges of regulated cell death: implications for therapy resistance in cancer. Cells. 2024;13:1083. https://doi.org/10.3390/cells13131083.
14. Sanz AB, Sanchez-Niño MD, Ramos AM, Ortiz A. Regulated cell death pathways in kidney disease. Nat Rev Nephrol. 2023;19:281–99. https://doi.org/10.1038/s41581-023-00694-0.
15. Hotchkiss RS, Strasser A, McDunn JE, Swanson PE. Cell death in disease: mechanisms and emerging therapeutic concepts. N Engl J Med. 2009;361:1570–83. https://doi.org/10.1056/NEJMra0901217.
16. Pentimalli F, Grelli S, Di Daniele N, Melino G, Amelio I. Cell death pathologies: targeting death pathways and the immune system for cancer therapy. Genes Immun. 2018;20:539.
17. Galluzzi L, Vitale I, Aaronson SA, Abrams JM, Adam D, Agostinis P, et al. Molecular mechanisms of cell death: recommendations of the nomenclature committee on cell death 2018. Cell Death Differ. 2018;25:486–541. https://doi.org/10.1038/s41418-017-0012-4.
18. Tang D, Kang R, Berghe TV, Vandenabeele P, Kroemer G. The molecular machinery of regulated cell death. Cell Res. 2019;29:347–64. https://doi.org/10.1038/s41422-019-0164-5.
19. Tsvetkov P, Coy S, Petrova B, Dreishpoon M, Verma A, Abdusamad M, et al. Copper induces cell death by targeting lipoylated TCA cycle proteins. Science. 2022;375:1254–61. https://doi.org/10.1126/science.abf0529.
20. Liu X, Nie L, Zhang Y, Yan Y, Wang C, Colic M, et al. Actin cytoskeleton vulnerability to disulfide stress mediates disulfidptosis. Nat Cell Biol. 2023;25:404–14. https://doi.org/10.1038/s41556-023-01091-2.
21. Zhou N, Bao J. FerrDb: a manually curated resource for regulators and markers of ferroptosis and ferroptosis-disease associations. Database. 2020;2020:baaa021. https://doi.org/10.1093/database/baaa021.
22. Gene Ontology Consortium, Aleksander SA, Balhoff J, Carbon S, Cherry JM, Drabkin HJ, et al. The Gene Ontology knowledgebase in 2023. Genetics. 2023;224:iyad031. https://doi.org/10.1093/genetics/iyad031.
23. Kanehisa M, Furumichi M, Sato Y, Matsuura Y, Ishiguro-Watanabe M. KEGG: biological systems database as a model of the real world. Nucleic Acids Res. 2025;53:D672–7. https://doi.org/10.1093/nar/gkae909.
24. Milacic M, Beavers D, Conley P, Gong C, Gillespie M, Griss J, et al. The Reactome Pathway Knowledgebase 2024. Nucleic Acids Res. 2024;52:D672–8. https://doi.org/10.1093/nar/gkad1025.
25. Zhou N, Yuan X, Du Q, Zhang Z, Shi X, Bao J, et al. FerrDb V2: update of the manually curated database of ferroptosis regulators and ferroptosis-disease associations. Nucleic Acids Res. 2023;51:D571–82. https://doi.org/10.1093/NAR/GKAC935.
26. Subramanian A, Tamayo P, Mootha VK, Mukherjee S, Ebert BL, Gillette MA, et al. Gene set enrichment analysis: a knowledge-based approach for interpreting genome-wide expression profiles. Proc Natl Acad Sci U S A. 2005;102:15545.
27. Zhou N, Peng L, Luo Q, Yin T, Sun H, Zhang Y, et al. FerrDb V3: expanding the manually curated resource for regulators and disease associations from ferroptosis to regulated cell death. Nucleic Acids Res. 2025;54:D572.
28. Zhao K, Rhee SY. Interpreting omics data with pathway enrichment analysis. Trends Genet. 2023;39:308–19. https://doi.org/10.1016/j.tig.2023.01.003.
29. Xie Z, Bailey A, Kuleshov MV, Clarke DJB, Evangelista JE, Jenkins SL, et al. Gene set knowledge discovery with enrichr. Curr Protoc. 2021;1:e90. https://doi.org/10.1002/cpz1.90.
30. Fang Z, Liu X, Peltz G. GSEApy: a comprehensive package for performing gene set enrichment analysis in Python. Bioinformatics. 2023;39:btac757. https://doi.org/10.1093/bioinformatics/btac757.
31. Koopmans F. GOAT: efficient and robust identification of gene set enrichment. Commun Biol. 2024;7:744. https://doi.org/10.1038/s42003-024-06454-5.

32. Pawel S, Roos M, Held L. Combined p-value functions for compatible effect estimation and hypothesis testing in drug regulation. Stat Med. 2025. https://doi.org/10.48550/arXiv.2503.10246
33. Zhu J, Wang Z, Li J, Kang D. Comprehensive analysis of regulated cell death in intracranial aneurysms. Front Biosci Landmark Ed. 2023;28:289. https://doi.org/10.31083/j.fbl2811289.
34. Kleinloog R, Verweij BH, van der Vlies P, Deelen P, Swertz MA, de Muynck L, et al. RNA sequencing analysis of intracranial aneurysm walls reveals involvement of lysosomes and immunoglobulins in rupture. Stroke. 2016;47:1286–93. https://doi.org/10.1161/STROKEAHA.116.012541.
35. Liu C, Zheng X, Ji J, Zhu X, Liu X, Liu H, et al. The carotenoid torularhodin alleviates NAFLD by promoting Akkermanisa muniniphila-mediated adenosylcobalamin metabolism. Nat Commun. 2025;16:3338. https://doi.org/10.1038/s41467-025-58500-3.
36. Huang DW, Sherman BT, Lempicki RA. Bioinformatics enrichment tools: paths toward the comprehensive functional analysis of large gene lists. Nucleic Acids Res. 2009;37:1–13. https://doi.org/10.1093/nar/gkn923.
37. Alhamdoosh M, Ng M, Wilson NJ, Sheridan JM, Huynh H, Wilson MJ, et al. Combining multiple tools outperforms individual methods in gene set enrichment analyses. Bioinformatics. 2017;33:414–24. https://doi.org/10.1093/bioinformatics/btw623.
38. Heard N, Rubin-Delanchy P. Choosing between methods of combining p-values. Biometrika. 2018;105:239–46. https://doi.org/10.1093/biomet/asx076.
39. Liu Y, Xie J. Cauchy combination test: a powerful test with analytic p-value calculation under arbitrary dependency structures. J Am Stat Assoc. 2020;115:393–402. https://doi.org/10.1080/01621459.2018.1554485.
40. Wijesooriya K, Jadaan SA, Perera KL, Kaur T, Ziemann M. Urgent need for consistent standards in functional enrichment analysis. PLoS Comput Biol. 2022;18:e1009935. https://doi.org/10.1371/journal.pcbi.1009935.
41. Li S, Zhang Q, Chen Z, Huang Z, Zhang L, Chen F. Novel insight into ferroptosis-related genes, molecular subtypes, and immune characteristics in intracranial aneurysms. Inflamm Res Off J Eur Histamine Res Soc Al. 2022;71:1347–64. https://doi.org/10.1007/s00011-022-01633-8.
42. Zhu H, Tan J, Wang Z, Wu Z, Zhou W, Zhang Z, et al. Bioinformatics analysis constructs potential ferroptosis-related ceRNA network involved in the formation of intracranial aneurysm. Front Cell Neurosci. 2022;16:1016682. https://doi.org/10.3389/fncel.2022.1016682.
43. Wu M, Zhang X, Zhang W, Chiou YS, Qian W, Liu X, et al. Cancer stem cell regulated phenotypic plasticity protects metastasized cancer cells from ferroptosis. Nat Commun. 2022;13:1371. https://doi.org/10.1038/s41467-022-29018-9.
44. Wang D, Chu WK, Yam JCS, Pang CP, Leung YC, Shum ASW, et al. GCN2-SLC7A11 axis coordinates autophagy, cell cycle and apoptosis and regulates cell growth in retinoblastoma upon arginine deprivation. Cancer Metab. 2024;12:31. https://doi.org/10.1186/s40170-024-00361-3.
45. Deng J-T, Wang X-L, Chen Y-X, O'Brien ER, Gui Y, Walsh MP. The effects of knockdown of rho-associated kinase 1 and zipper-interacting protein kinase on gene expression and function in cultured human arterial smooth muscle cells. PLoS ONE. 2015;10:e0116969. https://doi.org/10.1371/journal.pone.0116969.
46. Rivera-Serrano M, Flores-Colón M, Valiyeva F, Meléndez LM, Vivas-Mejía PE. Upregulation of MMP3 promotes cisplatin resistance in ovarian cancer. Int J Mol Sci. 2025;26:4012. https://doi.org/10.3390/ijms26094012.

Publisher's note